Half sandwich platinum group metal complexes containing tetradentate N-donor ligand bearing two pyrazolyl-pyridine units linked by an aromatic spacer

Gajendra Gupta [a], Bruno Therrien [b], Kollipara Mohan Rao [a,*]

[a] Department of Chemistry, North Eastern Hill University, Shillong 793022, India
[b] Service Analytique Facultaire, Université de Neuchâtel, Case Postale 158, CH-2009 Neuchâtel, Switzerland

ARTICLE INFO

ABSTRACT

Reaction of the bis-bidentate ligand, 1,3-bis((3-(pyridin-2-yl)-1H-pyrazol-1-yl)methyl)benzene ($NN \cap NN$), containing two chelating pyrazolyl-pyridine units connected by an aromatic spacer with platinum group metal complexes results in a series of cationic binuclear complexes, $[(\eta^6\text{-arene})_2Ru_2(NN \cap NN)Cl_2]^{2+}$ (arene = C_6H_6, **1**; $p\text{-}^iPrC_6H_4Me$, **2**; C_6Me_6, **3**), $[(\eta^5\text{-}C_5Me_5)_2M_2(NN \cap NN)Cl_2]^{2+}$ (M = Rh, **4**; Ir, **5**), $[(\eta^5\text{-}C_5H_5)_2M_2(NN \cap NN)(PPh_3)_2]^{2+}$ (M = Ru, **6**; Os, **7**), $[(\eta^5\text{-}C_5Me_5)_2Ru_2(NN \cap NN)(PPh_3)_2]^{2+}$ (**8**) and $[(\eta^5\text{-}C_9H_7)_2Ru_2(NN \cap NN)(PPh_3)_2]^{2+}$ (**9**). All these complexes have been isolated as their hexafluorophosphate salts and fully characterized by use of a combination of NMR spectroscopy, IR spectroscopy and mass spectrometry. The solid state structures of three complexes, $[2][PF_6]_2$, $[4][PF_6]_2$ and $[6][PF_6]_2$, has been determined by X-ray crystallographic studies.

© 2009 Elsevier B.V. All rights reserved.

1. Introduction

The synthesis of metal complexes with multiple coordination domains is an area of significant current interest in organometallic chemistry. Such complexes have been prepared as part of studies in diverse areas such as inter-metallic communication [1], bioinorganic enzyme active site modeling [2], supramolecular approaches to chiral materials [3] and functional devices [4]. The organometallic chemistry of half-sandwich complexes have been broadly developed in the past few decades, due to their wide range of potential applications as catalyst precursors for hydrogen transfer [5,6], ring opening metathesis polymerization [7,8] and olefin oxidation [9]. Arene ruthenium compounds have also been extensively investigated for their persuasive antibacterial and anticancer activity [10,11]. The arene confers great stability to ruthenium in the +2 oxidation state and the characteristic "piano stool" structure offers the possibility to vary the additional donors via substitution of halide(s) with a variety of σ-donors ranging from tertiary phosphines [12] to β-diketones [13] to aliphatic as well as aromatic amines [14–16].

We describe in this paper the coordination chemistry of the tetradentate nitrogen donor ligand, 1,3-bis((3-(pyridin-2-yl)-1H-pyrazol-1-yl)methyl)benzene ($NN \cap NN$), in which the two pyrazolyl-pyridine units are connected by an aromatic spacer. Although extensive studies have been carried out in the preparation of polyhedral cages of Cu, Ag, Ni and other metal complexes of pyraz-olyl-pyridine ligands by varying the spacer units, dinuclear complexes of platinum group metals with $NN \cap NN$ have not yet been investigated. This ligand has the ability to form both mono and dinuclear complexes with metals like Cu [17,18] and Ag [18], but surprisingly in the case of arene ruthenium and Cp*rhodium and Cp*iridium systems, it only forms dinuclear complexes. Herein, we describe the syntheses of nine dinuclear η^5 and η^6-cyclic π-perimeter hydrocarbon platinum group metal complexes bearing the ligand $NN \cap NN$. The complexes are characterized by a combination of NMR spectroscopy, IR spectroscopy, mass spectrometry and UV–Vis spectroscopy. The solid state structures of three complexes are determined by single crystal X-ray crystallographic studies. The ligand used in this study is in Scheme 1.

2. Results and discussion

2.1. Dinuclear arene ruthenium, rhodium and iridium complexes 1–5

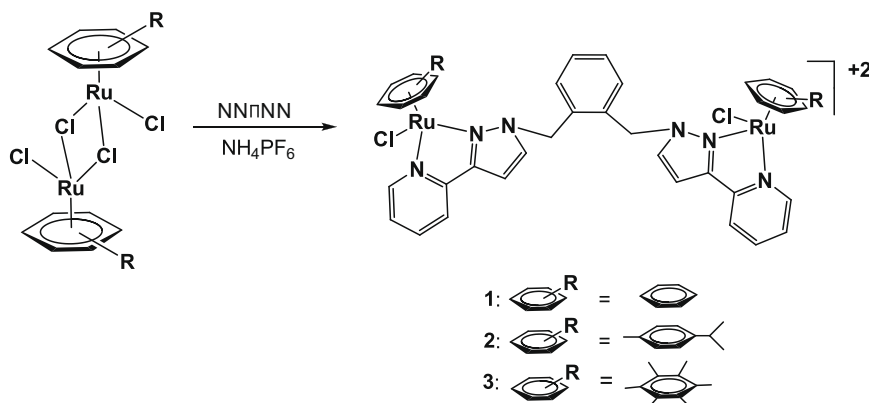The dinuclear arene ruthenium complexes $[(\eta^6\text{-arene})Ru(\mu\text{-Cl})Cl]_2$ react with the $NN \cap NN$ tetradentate pyrazolyl-pyridine ligand in
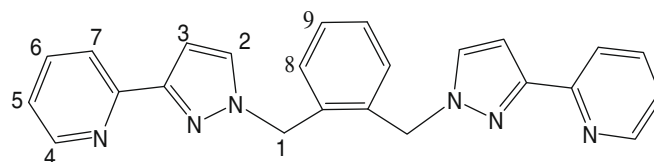
Scheme 1. $NN \cap NN$ tetradentate ligand used in this study.

Scheme 2.

methanol to afford the cationic dinuclear complexes [(η⁶-arene)₂Ru₂(NN∩NN)Cl₂]²⁺ (arene = C₆H₆, **1**; *p*-^{i}PrC₆H₄Me, **2**; C₆Me₆, **3**), isolated as their hexafluorophosphate salts (Scheme 2). Compounds [**2**][PF₆]₂ and [**3**][PF₆]₂ are yellow in color, while [**1**][PF₆]₂ is brown. These salts are non-hygroscopic and stable in air as well as in solution. They are sparingly soluble in polar solvents like dichloromethane, chloroform, acetone and acetonitrile but are insoluble in non-polar solvents like hexane, diethylether and petroleum ether. All compounds are characterized by ¹H NMR spectroscopy, IR spectroscopy and mass spectrometry. In the mass spectra, they show the expected molecular ion peaks *m/z* at 821.5, 933.8 and 990.7, corresponding to compounds [(η⁶-arene)₂Ru₂(NN∩NN)Cl₂]²⁺ (arene = C₆H₆, **1**; *p*-^{i}PrC₆H₄Me, **2**; C₆Me₆, **3**). All these halogenated complexes also displayed prominent peaks corresponding to the loss of both chloride ions from the molecular ion peak [M-(PF₆)₂]⁺, but the loss of arene group is not observed indicating the stronger bond of metal to arene group. The IR spectra of these complexes exhibit a sharp bands due to chelated NN∩NN tetradentate ligand in between 1616 and 1400 cm⁻¹ corresponding to the different stretching frequencies of C=C and C=N bond of these complexes as mentioned in Section 4. In the proton NMR spectra of **1**–**3**, the ligand peaks spread to the downfield region as compared to that of the free ligand. The free ligand exhibits two doublets at around δ 7.94–8.62 ppm for protons H4 and H7. However, after metallation, these doublets are shifted downfield in the range δ 8.15–9.51 ppm. In addition to the other ligand peaks as mentioned in Section 4, the ¹H NMR spectrum of complex **2** exhibit four doublets in the range of δ 6.16–5.71 ppm corresponding to the aromatic *p*-cymene ring of the CH protons. It also exhibits a singlet at δ 2.26 ppm, a pair of doublets at δ 0.95 and δ 1.05 ppm and a septet at δ 2.71 ppm for the protons of the methyl and isopropyl groups of the *p*-cymene ligands. However, in the case of **1**, the proton NMR spectrum displays a singlet at δ 6.25 ppm which corresponds to the protons of the benzene groups of the complex. The proton NMR spectrum of complex **3** exhibits a strong peak at δ 2.17 ppm for the hexamethylbenzene ligand, which is slightly shifted downfield in comparison to the starting complex [(η⁶-C₆Me₆)Ru(μ-Cl)Cl]₂. The molecular structure of representative complex **2** is solved by single crystal X-ray diffraction study and the structure is discussed later (Fig. 1).

The reaction of the dimeric chloro complexes [(η⁵-C₅Me₅)M(μ-Cl)Cl]₂ (M = Rh or Ir) with 1 equiv. of tetradentate ligand NN∩NN in methanol results in the formation of the yellow colored, air stable dicationic dinuclear complexes [(η⁵-C₅Me₅)₂Rh₂(NN∩NN)Cl₂]²⁺ (**4**) and [(η⁵-C₅Me₅)₂Ir₂(NN∩NN)Cl₂]²⁺ (**5**) which are isolated as their hexafluorophosphate salts (Scheme 3). Complexes **4** and **5** are characterized by ¹H NMR spectroscopy, IR spectroscopy and mass spectrometry. The infrared spectra of both the complexes exhibit
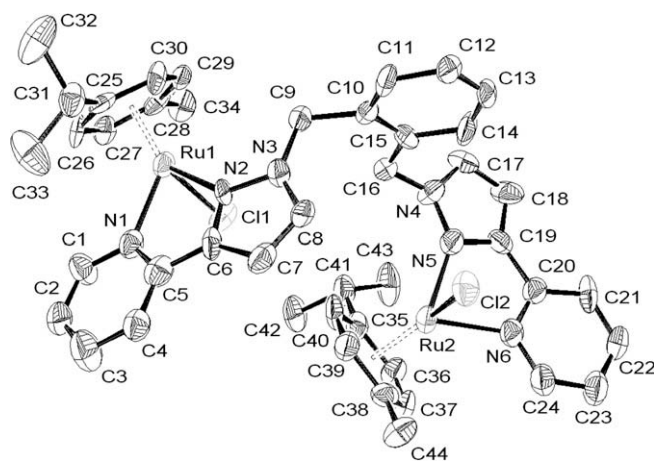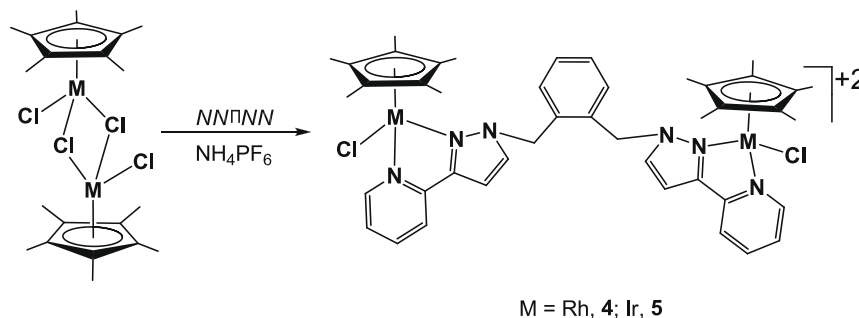

Fig. 1. Molecular structure of [(η⁶-*p*-^{i}PrC₆H₄Me)₂Ru₂(NN∩NN)Cl₂](PF₆)₂ at 35% probability level. Hydrogen atoms, dichloromethane molecule and hexafluorophosphate anions have been omitted for clarity.

a sharp bands due to bis-chelating NN∩NN ligand in between 1624 and 1400 cm⁻¹ corresponding to the stretching frequencies of C=C and C=N bond of these complexes. The ¹H NMR spectra of these complexes show ligand peaks a downfield shift in the position of signals associated with protons of ligand NN∩NN compared to that of the uncoordinated ligand suggesting coordination of the nitrogen atoms to the metal center in a bidentate fashion. In the ¹H NMR spectra of complexes **1**–**3** and **5**–**9** exhibit a singlet in the range of δ 6.91 and δ 5.49 ppm corresponding to the CH₂ protons of the ligand, but surprisingly, in compound **4** (see NMR spectrum of this complex in Supplementary material) these two CH₂ protons are diastereotopic and give rise to two doublets at approximately δ 5.9 ppm and δ 5.7 ppm for the four protons with a geminal coupling constant of 14 Hz. Besides this, the ¹H NMR spectra of these complexes display a singlet at around δ 1.66 and δ 1.56 ppm corresponding to the protons of the pentamethylcyclopentadienyl groups. The *m/z* values of all these complexes and their stable ion peaks obtained from the ESI mass spectra, as listed in Section 4, which are in good agreement with the theoretically expected values. ESI mass spectra of the complexes also displayed prominent peaks corresponding to the molecular ion fragment. These halogenated complexes displayed the prominent peak corresponding to the loss of chloride ion from the molecular ion peak, but the loss of Cp* group is not observed indicating the stronger bond of metal to this group and remains intact. The molecular structure of representative compound **4** is
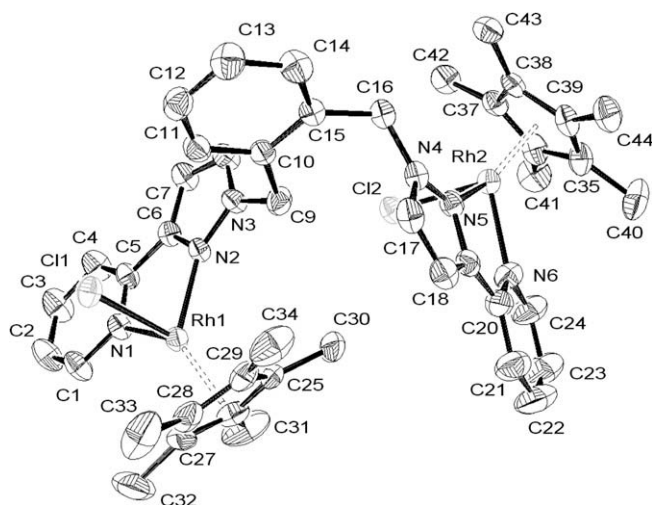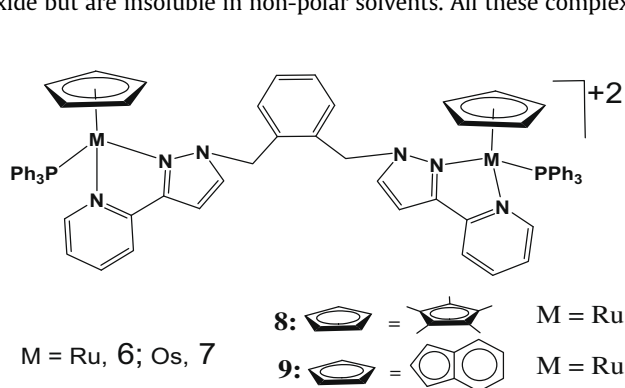
Scheme 3.

M = Rh, **4**; Ir, **5**

Fig. 2. Molecular structure of $[(\eta^5\text{-}C_5Me_5)_2Rh_2(NN\cap NN)Cl_2](PF_6)_2$ at 35% probability level. Hydrogen atoms, water molecules and hexafluorophosphate anions have been omitted for clarity.

solved by single crystal X-ray diffraction study and the structure is discussed later (Fig. 2).

2.2. Dinuclear cyclopentadienyl ruthenium and osmium complexes 6–9

Two equivalents of mononuclear cyclopentadienyl complexes $[(Cp)M(PPh_3)_2Cl]$ (M = Ru, Os; Cp = $\eta^5\text{-}C_5H_5$, $\eta^5\text{-}C_9H_7$, $\eta^5\text{-}C_5Me_5$) react with tetradentate ligand $NN\cap NN$ in refluxing methanol to give the corresponding dinuclear complexes **6–9** which are isolated as their hexafluorophosphate salts (Scheme 4). The cationic complexes **6–9** are soluble in halogenated solvents and polar organic solvents such as tetrahydrofuran, methanol or dimethylsulfoxide but are insoluble in non-polar solvents. All these complexes

are stable in solid state as well as in solution. All complexes were characterized by IR spectroscopy, ^1H NMR spectroscopy, ^{31}P {^1H} NMR spectroscopy and mass spectrometry. The analytical data of these compounds are consistent with the formulations. Besides the IR bands as mentioned in Section 4, these complexes also display a strong band between 842 and 847 cm^{-1} due to the ν_{P-F} stretching frequency of the counter ion of these complexes. The ^1H and ^{31}P {^1H} NMR spectra of complexes were recorded in CDCl$_3$ and spectral data are summarized in Section 4. Shift in the position of signals associated with protons of ligand $NN\cap NN$, suggested coordination of nitrogen atom to the metal centre ruthenium and osmium in bi-dentate fashion. The protons of the ligand in these complexes **6–9** show downfield shift with respect to the protons of the uncoordinated ligand. The ^1H NMR spectrum of the uncoordinated ligand displays two doublets at δ 8.62 and δ 7.94 ppm for protons H4 and H7, whereas in the case of the metal complexes this doublet shifts to the downfield region between δ 9.31 and δ 8.34 ppm. In addition to the aromatic protons mentioned in Section 4, complexes **6** and **7** shows a singlet at δ 4.66 and δ 4.59 ppm which corresponds to the protons of the cyclopentadienyl ligand, while in the case of complex **8** it displays a singlet at δ 2.03 ppm corresponding to the methyl protons of the pentamethylcyclopentadienyl ligand. These complexes also show multiplets in the range of δ 6.8–7.4 ppm due to the protons of the coordinated triphenylphosphine ligands. Complex **9** exhibits three sets of signals, triplet at around δ 4.43 ppm, doublets at δ 4.97 ppm and δ 4.85 ppm corresponding to the protons of the indenyl group. The protons of the triphenylphosphine ligands exhibit a large multiplet centered at δ 7.32 ppm. In the ^{31}P {^1H} NMR spectra of the complexes **6**, **8** and **9**, the ^{31}P nuclei of the coordinated PPh$_3$ resonated as a sharp singlet in the range of δ 57.1–49.6 ppm, respectively, whereas in the starting precursors the signal appears in the upfield region. In the case of complex **7** the ^{31}P {^1H} NMR spectrum displays a sharp singlet at δ −0.26 ppm as compared to the starting complex which is found at δ −6.29 ppm. The m/z values of all these

Scheme 4.

M = Ru, **6**; Os, **7**

8: ⬡ = ⬠   M = Ru
9: ⬡ = ⬡⬡   M = Ru
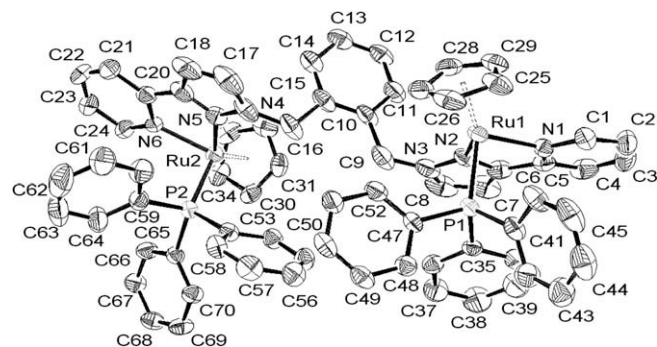
Fig. 3. Molecular structure of $[(\eta^5\text{-}C_5H_5)_2Ru_2(NN\cap NN)(PPh_3)_2](PF_6)_2$ at 35% probability level. Hydrogen atoms, diethyl ether molecule and hexafluorophosphate anions have been omitted for clarity.

complexes and their stable ion peaks obtained from the ZQ mass spectra, as listed in Section 4 and are in good agreement with the theoretically expected values. ESI mass spectra of the complexes also displayed prominent peaks corresponding to the molecular ion fragment. The structure of representative compound **6** was solved by single crystal X-ray diffraction study and is presented in Fig. 3.

2.3. Molecular structures of complexes [2](PF₆)₂·CH₂Cl₂, [4](PF₆)₂·2 H₂O and [6](PF₆)₂·0.5 Et₂O

The molecular structures of compounds [**2**](PF₆)₂, [**4**](PF₆)₂ and [**6**](PF₆)₂ are shown in Figs. 1–3, respectively, and selected bond lengths and angles are presented in Table 1. Complexes **2**, **4** and **6** contain two chiral Ru(II) or Rh(III) metal centers bonded to a η^6-p-^{i}PrC₆H₄Me or η^5-C₅H₅ and η^5-C₅Me₅ ligands, respectively, which are bridged by the *NN∩NN* ligand through four nitrogen atoms. Therefore, two five-membered metallacycles are formed upon coordination of *NN∩NN* to the half-sandwich platinum group metals, with a N–M–N bite angle ranging from 74.4(4) to 76.1(4)°. Despite the presence of two chiral centers in **2**, **4** and **6**, only racemic mixtures were obtained, and all compounds crystallize in centrosymmetric space groups.

In the dinuclear complexes **2** and **4**, the two metal centers are more than 7 Å apart, while in **6** the Ru–Ru separation is more than 9 Å. This difference is probably due to the presence of the sterically demanding triphenylphosphine ligands in **6** as compared to the small chlorido ligands in **2** and **4**. The angles observed between the two planes formed by the coordinated pyridine-pyrazolyl units are 47.5(2)° in **2**, 74.7(1)° in **4** and 29.6(1)° in **6**, thus suggesting a great flexibility of the *NN∩NN* chelating ligand. Indeed, as emphasized in Fig. 4, the angles found between the least-square plane of the central –CH₂–Ph–CH₂– group and the pyridine-pyrazolyl planes are all comprised between 77.0(1)° and 89.5(1)°.

The presence of solvent molecules and of hexafluorophosphate anions in the crystal packing of [**2**](PF₆)₂·CH₂Cl₂, [**4**](PF₆)₂·2 H₂O and [**6**](PF₆)₂·0.5 Et₂O gives rise to multiple hydrogen bonds and short contacts which are all showing of standard distances and angles.

Space filling views of the *NN∩NN*-M₂ moieties in **2**, **4** and **6** (Fig. 4) and colored representations of the planes formed by the central phenyl (green) and the two pyridine-pyrazolyl units (red and blue) to emphasize the structural flexibility of the *NN∩NN* ligand. (For color combination see Supplementary material.)

2.4. UV–Vis spectroscopy

UV–Vis spectra of the complexes **1–6** and **8** were acquired in acetonitrile and spectral data are summarized in Table 2. Electronic

spectra of representative complexes are depicted in Fig. 5. The low spin d^6 configuration of these dinuclear complexes provides filled orbitals of proper symmetry at the Ru(II) centers which can interact with the low lying π^* orbital of the ligands. One should therefore expect a band attributable to the metal-to-ligand charge transfer (MLCT) $t_{2g} \rightarrow \pi^*$ transition in their electronic spectra [19–24]. The electronic spectra of these complexes display a medium intensity band in the UV–Vis region. The lowest energy absorption bands in the electronic spectra of these complexes in the visible region ∼420–408 and ∼395–345 nm have been tentatively assigned on the basis of their intensity and position to $t_{2g} \rightarrow \pi^*$ MLCT transitions. The bands on the high energy side at ∼300–235 nm for the complexes **1–6** and **8**, have been assigned to ligand-centered $\pi \rightarrow \pi^*/n \rightarrow \pi^*$ transitions [25,26]. In general, these complexes follow the normal trends observed in the electronic spectra of the nitrogen-bonded metal complexes, which display a ligand-based $\pi \rightarrow \pi^*$ transition for pyrazolyl pyridazine ligands in the UV region and metal-to-ligand charge transfer transitions in the visible region.

3. Conclusions

In summary, a series of new dinuclear η^5-and η^6-cyclic π-perimeter hydrocarbon metal complexes bearing ligand *NN∩NN*, which are remarkably stable in the solid state and in solution have been successfully synthesized in good yield. All these complexes have been fully characterized by a combination of NMR spectroscopy, IR spectroscopy, UV–Vis spectroscopy and mass spectrometry. The ligand has ability to form both mononuclear and dinuclear complexes by variation of metal–ligand ratio, however arene ruthenium and Cp*Rh and Cp*Ir reactions yielded dinuclear complexes only.

4. Experimental

4.1. Physical measurements

Infrared spectra were recorded on a Perkin–Elmer Model 983 spectrophotometer with the sample prepared as KBr pellets. The NMR spectra were obtained using Bruker Advance II 400 spectrometer in CD₃CN, CDCl₃ and Acetone-d_6, respectively, for complexes using TMS as an internal standard. Mass spectra were obtained from a Waters ZQ – 4000 mass spectrometer by the ESI method. All chemicals used were of reagent grade. Elemental analyses of the complexes were performed on a Perkin–Elmer 2400 CHN/S analyzer. All reactions were carried out in distilled and dried solvents. The ligand *NN∩NN* was prepared by following a literature procedure [17]. The precursor complexes [(η^6-arene)Ru(μ-Cl)Cl]₂ (arene = C₆H₆, p-^{i}PrC₆H₄Me and C₆Me₆), [(η^5-C₅Me₅)M(μ-Cl)Cl]₂ (M = Rh, Ir) [27–31], [(η^5-C₅H₅)Ru(PPh₃)₂Cl], [(η^5-C₅H₅)Os-

Table 1
Selected bond lengths (Å) and angles (°) for [**2**](PF₆)₂·CH₂Cl₂, [**4**](PF₆)₂·2 H₂O and [**6**](PF₆)₂·0.5 Et₂O.

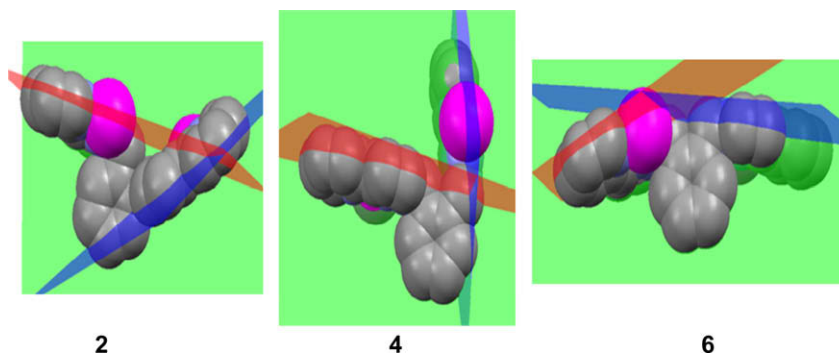|	[**2**](PF₆)₂		[**4**](PF₆)₂		[**6**](PF₆)₂	
	Ru1	Ru2	Rh1	Rh2	Ru1	Ru2
Distances (Å)						
M–N$_{pyr}$	2.099(11)	2.152(9)	2.134(3)	2.124(4)	2.110(3)	2.099(3)
M–N$_{prz}$	2.120(9)	2.074(11)	2.124(3)	2.143(3)	2.094(3)	2.125(2)
M–Cl	2.386(3)	2.412(3)	2.384(1)	2.398(1)		
M–P					2.3413(9)	2.3172(9)
M–M	7.195(1)		7.4794(6)		9.0293(4)	
Angles (°)						
N$_{pyr}$–M–N$_{prz}$	74.4(4)	76.1(4)	75.78(13)	75.48(14)	75.29(11)	75.30(11)
N$_{pyr}$–M–Cl	86.7(3)	87.2(3)	86.93(10)	87.81(11)		
N$_{prz}$–M–Cl	83.6(3)	85.4(3)	87.39(10)	89.81(9)		
N$_{pyr}$–M–P					92.07(8)	92.98(8)
N$_{prz}$–M–P					88.61(8)	89.01(9)

Fig. 4. Space filling views of the $NN \cap NN$-M_2 moieties in **2**, **4** and **6**, and colored representations of the planes formed by the central phenyl (green) and the two pyridine-pyrazolyl units (red and blue) to emphasize the structural flexibility of the $NN \cap NN$ ligand. (For color combination see Supplementary material.) (For interpretation of the references to colour in this figure legend, the reader is referred to the web version of this article.)

Table 2
UV–Vis absorption data in acetonitrile at 298 K.

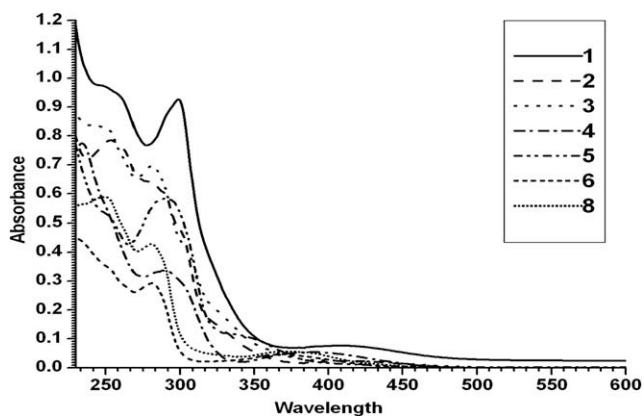| Complex	λ_{max}/nm ($\varepsilon/10^{-4}$ M^{-1} cm^{-1})		
1	250(0.97)	300(0.92)	420(0.11)
2	258(0.78)	285(0.63)	408(0.04)
3	255(0.83)	280(0.69)	410(0.05)
4	235(0.77)	291(0.33)	395(0.07)
5	253(0.52)	297(0.58)	345(0.12)
6	252(0.35)	283(0.28)	380 (0.07)
8	253 (0.58)	282(0.43)	382(0.08)

Fig. 5. UV–Vis absorption spectra of dinuclear complexes **1** to **6** and **8** in acetonitrile at 298 K.

(PPh$_3$)$_2$Br], [(η^5-C$_5$Me$_5$)Ru(PPh$_3$)$_2$Cl] and [(η^5-C$_9$H$_7$)Ru(PPh$_3$)$_2$Cl] were prepared by following the literature methods [32–36].

4.2. Single-crystal X-ray structures analyses

Crystals of [**2**](PF$_6$)$_2$·CH$_2$Cl$_2$ were grown from dichloromethane/petroleum ether as small orange plates. Crystals of [**4**](PF$_6$)$_2$·H$_2$O and [**6**](PF$_6$)$_2$·0.5 Et$_2$O were grown by slow diffusion of petroleum ether into a wet acetone solution of the respective complexes as deep red blocks. The crystallizations were done at room temperature. Crystals of complexes [**2**](PF$_6$)$_2$, [**4**](PF$_6$)$_2$ and [**6**](PF$_6$)$_2$ were mounted on a Stoe Image Plate Diffraction system equipped with a ϕ circle goniometer, using Mo Kα graphite monochromated radiation ($\lambda = 0.71073$ Å) with ϕ range 0–200°. The structures were solved by direct methods using the program SHELXS-97 [37]. Refinement and all further calculations were carried out using SHELXL-97

[37]. The H-atoms were included in calculated positions and treated as riding atoms using the SHELXL default parameters. The non-H atoms were refined anisotropically, using weighted full-matrix least-square on F^2. In [**4**](PF$_6$)$_2$·H$_2$O and [**6**](PF$_6$)$_2$·0.5 Et$_2$O disordered solvent molecules were found and not refined anisotropically, while in [**2**](PF$_6$)$_2$·CH$_2$Cl$_2$, the CH$_2$Cl$_2$ was well defined and refined anisotropically. Crystallographic details are summarized in Table 3. Figures of the complexes were drawn with ORTEP-32 [38].

4.3. Preparation of [(η^6-arene)$_2$M$_2$($NN \cap NN$)Cl$_2$](PF$_6$)$_2$ {M = Ru, arene = C$_6$H$_6$ [**1**](PF$_6$)$_2$, η^6-p-^{i}PrC$_6$H$_4$Me [**2**](PF$_6$)$_2$, C$_6$Me$_6$ [**3**](PF$_6$)$_2$, M = Rh, arene = C$_5$Me$_5$ [**4**](PF$_6$)$_2$ and M = Ir, arene = C$_5$Me$_5$ [**5**](PF$_6$)$_2$}

A mixture of [(η^6-arene)M(μ-Cl)Cl]$_2$ (M = Ru, Rh and Ir) (0.10 mmol), $NN \cap NN$ (40 mg, 0.10 mmol) and 2 equiv. of NH$_4$PF$_6$ was stirred in dry methanol (30 ml) for 4 h at room temperature. The yellow compound which formed was filtered, washed with ethanol, diethyl ether and dried under vacuum.

Compound [**1**](PF$_6$)$_2$: Yield: 102 mg, 81.7%. Elemental Anal. Calc. for C$_{36}$H$_{32}$Cl$_2$F$_{12}$N$_6$P$_2$Ru$_2$: C, 38.93; H, 2.92; N, 7.57. Found: C, 39.21; H, 3.08; N, 7.32%. IR (KBr pellets, cm^{-1}): 1616 (m), 1442 (s), 843 (s), 771 (s), 558 (s). IR (CsI pellets, cm^{-1}): 274 (s); ^{1}H NMR (400 MHz, CD$_3$CN): δ = 9.48 (d, 2H), 8.15 (d, J = 7.4 Hz, 2H), 7.90 (d, J = 8 Hz, 2H), 7.62 (q, 6H), 6.32 (s, 4H, –CH$_2$), 6.253 (s, 12H, C$_6$H$_6$), 5.98–5.82 (m, 4H); ESI-MS (m/z): 821.5 [M-(PF$_6$)$_2$]$^+$, 863.3 [M-(PF$_6$)$_2$-Cl$_2$]$^+$.

Compound [**2**](PF$_6$)$_2$: Yield: 90 mg, 79.3%. Elemental Anal. Calc. for C$_{44}$H$_{48}$Cl$_2$F$_{12}$N$_6$P$_2$Ru$_2$: C, 43.22; H, 3.95; N, 6.89. Found: C, 43.45; H, 4.11; N, 6.71. IR (KBr pellets, cm^{-1}): 1616 (m), 1439 (s), 843 (s), 773 (s), 558 (s). IR (CsI pellets, cm^{-1}): 279 (s); ^{1}H NMR (400 MHz, Acetone-d_6): δ = 9.51 (d, J = 6 Hz, 2H), 8.57 (d, J = 4.4 Hz, 2H), 8.30 (dt, J = 4.4 Hz, 2H), 7.97 (d, J = 6.4 Hz, 2H), 7.94–7.24 (m, 6H), 6.91 (s, 4H, –CH$_2$), 6.45 (d, J = 6 Hz, 2H), 6.16(d, J = 5.6 Hz, 2H, Ar$_{p-cy}$), 6.04 (d, J = 6 Hz, 2H, Ar$_{p-cy}$), 5.89 (d, J = 5.2 Hz, 2H, Ar$_{p-cy}$), 5.71 (d, J = 6 Hz, 2H, Ar$_{p-cy}$), 2.71 (sep, 2H), 2.29 (s, 3H), 2.26 (s, 3H), 1.05 (dd, J = 7.2 Hz, 6H), 0.95 (d, J = 7.2 Hz, 6H); ESI-MS (m/z): 933.8 [M-(PF$_6$)$_2$]$^+$, 750.7 [M-(PF$_6$)$_2$-Cl$_2$]$^+$.

Compound [**3**](PF$_6$)$_2$: Yield: 101 mg, 77.4%. Elemental Anal. Calc. for C$_{48}$H$_{56}$Cl$_2$F$_{12}$N$_6$P$_2$Ru$_2$: C, 45.07; H, 4.41; N, 6.59. Found: C, 45.32; H, 4.55; N, 6.37%. IR (KBr pellets, cm^{-1}): 1624 (m), 1384 (s), 847 (s), 775 (s), 561 (s). IR (CsI pellets, cm^{-1}): 288 (s); ^{1}H NMR (400 MHz, CDCl$_3$): δ = 9.41 (d, J = 7.2 Hz, 2H), 8.96 (d, J = 8 Hz, 2H), 8.73 (d, J = 8 Hz, 2H), 8.42 (q, 6H), 6.11 (s, 4H, –CH$_2$), 5.78–5.61 (m, 4H), 2.17 (s, 36H, C$_6$Me$_6$); ESI-MS (m/z): 990.7 [M-(PF$_6$)$_2$]$^+$, 919.4 [M-(PF$_6$)$_2$-Cl$_2$]$^+$.

Table 3
Crystallographic and structure refinement parameters for complexes [2](PF$_6$)$_2$·CH$_2$Cl$_2$, [4](PF$_6$)$_2$·2 H$_2$O and [6](PF$_6$)$_2$·0.5 Et$_2$O.

	[2](PF$_6$)$_2$	[4](PF$_6$)$_2$	[6](PF$_6$)$_2$
Chemical formula	C$_{45}$H$_{50}$Cl$_4$F$_{12}$N$_6$P$_2$Ru$_2$	C$_{44}$H$_{54}$Cl$_2$F$_{12}$N$_6$O$_2$P$_2$Rh$_2$	C$_{71}$H$_{62.5}$F$_{12}$N$_6$O$_{0.5}$P$_4$Ru$_2$
Formula weight	1308.79	1265.59	1561.79
Crystal system	monoclinic	monoclinic	monoclinic
Space group	P2$_1$/c (no. 14)	P2$_1$/n (no. 14)	P2$_1$/c (no. 14)
Crystal color and shape	orange block	red block	red block
Crystal size	0.24 × 0.18 × 0.16	0.28 × 0.23 × 0.18	0.33 × 0.23 × 0.20
a (Å)	23.4756(11)	14.0140(12)	14.0334(3)
b (Å)	12.2948(7)	13.1382(7)	17.2822(5)
c (Å)	18.9077(11)	29.572(2)	28.2555(6)
β (°)	110.810(6)	100.209(9)	96.182(2)
V (Å^3)	5101.3(5)	5358.6(7)	6812.9(3)
Z	4	4	4
T (K)	173(2)	173(2)	173(2)
D$_c$ (g cm^{-3})	1.704	1.569	1.523
μ (mm^{-1})	0.948	0.858	0.618
Scan range (°)	2.04 < θ < 26.06	2.09 < θ < 26.04	1.87 < θ < 29.20
Unique reflections	10 043	10 516	18 392
Reflections used [I > 2σ(I)]	2509	7081	9707
R$_{int}$	0.2202	0.0465	0.0865
Final R indices [I > 2σ(I)][a]	0.0563, wR$_2$ 0.0860	0.0467, wR$_2$ 0.1170	0.0415, wR$_2$ 0.0829
R indices (all data)	0.2315, wR$_2$ 0.1268	0.0711, wR$_2$ 0.1252	0.1037, wR$_2$ 0.0957
Goodness-of-fit	0.617	0.897	0.805
Max, Min Δρ (e Å^{-3})	0.559, −1.000	0.968, −0.739	1.251, −0.491

[a] Structures were refined on F_o^2: $wR_2 = [\sum[w(F_o^2 - F_c^2)^2]/\sum w(F_o^2)^2]^{1/2}$, where $w^{-1} = [\sum(F_o^2) + (aP)2 + bP]$ and $P = [\max(F_o^2, 0) + 2F_c^2]/3$.

Compound [4](PF$_6$)$_2$: Yield: 103 mg, 82.1%. Elemental Anal. Calc. for C$_{44}$H$_{50}$Cl$_2$F$_{12}$N$_6$P$_2$Rh$_2$: C, 43.01; H, 4.12; N, 6.86. Found: C, 43.23; H, 4.33; N, 6.71%. IR (KBr pellets, cm^{-1}): 1615 (m), 1444 (s), 845 (s), 770 (s), 558 (s); ^{1}H NMR (400 MHz, Acetone-d$_6$): δ = 9.04 (d, J = 5.6 Hz, 2H), 8.33 (dd, J = 6.4 Hz, 4H), 7.96 (d, J = 2.8 Hz, 2H), 7.848 (dt, J = 4 Hz, 2H), 7.59–7.39 (m, 6H), 5.98 (d, J = 14 Hz, 2H, –CH$_2$), 5.68 (d, J = 14.4 Hz, 2H, –CH$_2$), 1.66 (s, 30H, C$_5$Me$_5$); ESI-MS (m/z): 940.3 [M-(PF$_6$)$_2$]$^+$, 869.2 [M-(PF$_6$)$_2$-Cl$_2$]$^+$.

Compound [5](PF$_6$)$_2$: Yield: 106 mg, 73.8%. Elemental Anal. Calc. for C$_{44}$H$_{50}$Cl$_2$F$_{12}$N$_6$P$_2$Ir$_2$: C, 37.55; H, 3.59; N, 5.99. Found: C, 37.72; H, 3.74; N, 5.82%. IR (KBr pellets, cm^{-1}): 1617 (m), 1446 (s), 842 (s), 770 (s), 558 (s); ^{1}H NMR (400 MHz, Acetone-d$_6$): δ = 8.73 (d, J = 5.6 Hz, 2H), 8.12 (d, J = 7.2 Hz, 4H), 7.66 (q, 4H), 7.520–7.381 (m, 6H), 5.57(s, 4H, –CH$_2$), 1.56 (s, 30H, C$_5$Me$_5$); ESI-MS (m/z): 1117.7 [M-(PF$_6$)$_2$]$^+$, 1047.3 [M-(PF$_6$)$_2$-Cl$_2$]$^+$.

4.4. Preparation of [(η^5-Cp)$_2$M$_2$(NN∩NN)(PPh$_3$)$_2$](PF$_6$)$_2$ {Cp = C$_5$H$_5$, M = Ru [6](PF$_6$)$_2$, Os [7](PF$_6$)$_2$, Cp = C$_5$Me$_5$, M = Ru [8](PF$_6$)$_2$ and Cp = C$_9$H$_7$, M = Ru [9](PF$_6$)$_2$}

A mixture of [(η^5-Cp)M(PPh$_3$)$_2$X] {M = Ru, X = Cl and M = Os, X = Br} (0.20 mmol), NN∩NN (40 mg, 0.10 mmol) and 2 equiv. of NH$_4$PF$_6$ in dry methanol (30 ml) were refluxed for 12 h until the color of the solution changed from pale yellow to orange. The solvent was removed under vacuum, the residue was dissolved in dichloromethane (10 ml), and the solution filtered to remove ammonium halide. The orange solution was concentrated to 5 ml, upon addition of diethylether the orange-yellow complex was precipitated, which was separated and dried under vacuum.

Compound [6](PF$_6$)$_2$: Yield: 103 mg, 65.6%. Elemental Anal. Calc. for C$_{70}$H$_{60}$F$_{12}$N$_6$P$_4$Ru$_2$: C, 54.64; H, 3.93; N, 5.45. Found: C, 54.79; H, 4.17; N, 5.33%. IR (KBr pellets, cm^{-1}): 1624 (m), 1437 (s), 842 (s), 776 (s), 558 (s); ^{1}H NMR (400 MHz, CDCl$_3$): δ = 9.00 (d, J = 5.6 Hz, 2H), 8.62 (d, J = 4.8 Hz, 2H), 8.56 (d, J = 4.8 Hz, 2H), 7.96–7.01 (m, 36H, PPh$_3$ and pyridyl and phenyl), 6.95 (t, J = 6.4 Hz, 2H), 6.63 (d, J = 2.8 Hz, 2H), 5.49 (s, 4H, –CH$_2$), 4.66 (s, 10H, C$_5$H$_5$); ESI-MS (m/z): 1248.4 [M-(PF$_6$)$_2$]$^+$; ^{31}P {^{1}H} NMR (CDCl$_3$, δ): 50.82 (s, PPh$_3$).

Compound [7](PF$_6$)$_2$: Yield: 109 mg, 62.2%. Elemental Anal. Calc. for C$_{70}$H$_{60}$F$_{12}$N$_6$P$_4$Os$_2$: C, 48.97; H, 3.53; N, 4.89. Found: C, 49.18; H, 3.75; N, 4.71%. IR (KBr pellets, cm^{-1}): 1615 (m), 1444 (s), 845 (s),

773 (s), 554 (s); ^{1}H NMR (400 MHz, CDCl$_3$): δ = 9.31 (d, J = 6.4 Hz, 2H), 8.69 (d, J = 6.2 Hz, 2H), 8.55 (d, J = 4.8 Hz, 2H), 7.83–7.11 (m, 36H, PPh$_3$ and pyridyl and phenyl), 7.10 (t, J = 7.2 Hz, 2H), 6.72 (d, J = 2.8 Hz, 2H), 5.55 (s, 4H, –CH$_2$), 4.59 (s, 10H, C$_5$H$_5$); ESI-MS (m/z): 1428.3 [M-(PF$_6$)$_2$]$^+$; ^{31}P {^{1}H} NMR (CDCl$_3$, δ): −0.26 (s, PPh$_3$).

Compound [8](PF$_6$)$_2$: Yield: 111 mg, 63.3%. Elemental Anal. Calc. for C$_{80}$H$_{80}$F$_{12}$N$_6$P$_4$Ru$_2$: C, 57.24; H, 4.80; N, 5.01. Found: C, 57.45; H, 4.98; N, 4.79%. IR (KBr pellets, cm^{-1}): 1617 (m), 1444 (s), 847 (s), 770 (s), 558 (s); ^{1}H NMR (400 MHz, CDCl$_3$): δ = 8.65 (d, J = 7.6 Hz, 2H), 8.34 (d, J = 8 Hz, 2H), 8.27 (d, J = 7.2 Hz, 2H), 7.21–7.09 (m, 36H, PPh$_3$ and pyridyl and phenyl), 7.84 (t, J = 6.4 Hz, 2H), 6.64 (d, J = 7.6 Hz, 2H), 5.75 (s, 4H, –CH$_2$), 2.03 (s, 30H, C$_5$Me$_5$). ESI-MS (m/z): 1390.6 [M-(PF$_6$)$_2$]$^+$. ^{31}P {^{1}H} NMR (CDCl$_3$, δ): 49.6 (s, PPh$_3$).

Compound [9](PF$_6$)$_2$: Yield: 107 mg, 64%. Elemental Anal. Calc. for C$_{78}$H$_{64}$F$_{12}$N$_6$P$_4$Ru$_2$: C, 57.17; H, 3.94; N, 5.14. Found: C, 57.39; H, 4.10; N, 5.03%. IR (KBr pellets, cm^{-1}): 1615 (m), 1442 (s), 842 (s), 773 (s), 558 (s); ^{1}H NMR (400 MHz, CDCl$_3$): δ = 9.22 (d, J = 5.6 Hz, 2H), 8.75 (d, J = 8 Hz, 2H), 8.67 (d, J = 4.4 Hz, 2H), 8.23 (t, J = 7.6 Hz, 2H), 7.55–7.10 (m, 48H), 6.82 (d, J = 6.4 Hz, 2H), 5.53 (s, 4H, –CH$_2$), 4.97 (d, J = 8 Hz, 2H), 4.85 (d, J = 7.6 Hz, 2H), 4.43 (t, J = 2.4 Hz, 2H). ESI-MS (m/z): 1349.7 [M-(PF$_6$)$_2$]. ^{31}P {^{1}H} NMR (CDCl$_3$, δ): 57.10 (s, PPh$_3$). ESI-MS (m/z): 719.1 [M-PF$_6$]$^+$.

Appendix A. Supplementary material

CCDC 753325, 753326 and 753327 contain the supplementary crystallographic data for [2](PF$_6$)$_2$·CH$_2$Cl$_2$, [4](PF$_6$)$_2$·2 H$_2$O and [6](PF$_6$)$_2$·0.5 Et$_2$O. These data can be obtained free of charge from The Cambridge Crystallographic Data Centre via www.ccdc.cam.ac.uk/data_request/cif. Supplementary data associated with this article can be found, in the online version, at doi:10.1016/j.jorganchem.2009.12.012.

References

[1] V. Balzani, A. Juris, M. Venturi, S. Campagna, S. Serroni, Chem. Rev. 96 (1996) 759.
[2] R.H. Holm, P. Kennepohl, E.I. Solomon, Chem. Rev. 96 (1996) 2239.
[3] M. Albrecht, Chem. Rev. 101 (2001) 3457;
    C. Piguet, G. Bernardinelli, G. Hopfgartner, Chem. Rev. 97 (1997) 2005.
[4] J.-C.G. Bünzli, C. Piguet, Chem. Rev. 102 (2002) 1897.
[5] J. Canivet, L. Karmazin-Brelot, G. Süss-Fink, J. Organomet. Chem. 690 (2005) 3202.
[6] S. Ogo, T. Abura, Y. Watanabe, Organometallics 21 (2002) 2964.
[7] S. Ogo, K. Uehara, T. Abura, Y. Watanabe, S. Fukuzumi, Organometallics 23 (2004) 3047.
[8] A.W. Stumpf, E. Saive, A. Demonceau, F.A. Noels, J. Chem. Soc., Chem. Commun. (1995) 1127.
[9] M.K. Tse, C. Döbler, S. Bhor, M. Klawonn, W. Mägerlein, H. Hugl, M. Beller, Angew. Chem., Int. Ed. 43 (2004) 5255.
[10] Y.K. Yan, M. Melchart, A. Habtemariam, P.J. Sadler, J. Chem. Commun. (2005) 4764, and references therein.
[11] W.H. Ang, P.J. Dyson, Eur. J. Inorg. Chem. (2006) 4003, and references therein.
[12] B. Therrien, Coord. Chem. Rev. 253 (2009) 493.
[13] F. Marchetti, C. Pettinari, R. Pettinari, A. Cerquetella, A. Cingolani, E.J. Chan, K. Kozawa, B.W. Skelton, A.H. White, R. Wanke, M.L. Kuznetsov, L.M.D.R.S. Martins, A.J.L. Pombeiro, Inorg. Chem. 46 (2007) 8245. and references therein.
[14] R.J. Restivo, G. Ferguson, J. Chem. Soc., Chem. Commun. (1973) 847.
[15] C.J. Jones, J.A. McCleverty, A.S. Rothin, J. Chem. Soc., Dalton Trans. (1986) 109.
[16] S. Bhambri, A. Bishop, N. Kaltsoyannis, D.A. Tocher, J. Chem. Soc., Dalton Trans. (1998) 3379.
[17] I.S. Tidmarsh, B.F. Taylor, M.J. Hardie, L. Russo, W. Clegg, M.D. Ward, New. J. Chem. 33 (2009) 366.
[18] S.P. Argent, H. Adams, T. Riss-Johannessen, J.C. Jaffery, L.P. Harding, O. Mamula, M.D. Ward, Inorg. Chem. 45 (2006) 3905.
[19] N. Goswami, R. Alberto, C.L. Barnes, S. Jurisson, Inorg. Chem. 35 (1996) 7546.
[20] R. Samanta, P. Munshi, B.K. Santra, N.K. Lokanath, M.A. Sridhar, J.S. Prasad, G.K. Lahiri, J. Organomet. Chem. 579 (1999) 311.
[21] P.K. Santra, C. Sinha, W.-J. Sheen, F.-L. Liao, T.-H. Lu, Polyhedron 20 (2001) 599.
[22] A.K. Ghosh, K.K. Kamar, P. Paul, S.-M. Peng, G.-H. Lee, S. Goswami, Inorg. Chem. 41 (2002) 6343.
[23] C. Das, A.K. Ghosh, C.-H. Hung, G.-H. Lee, S.-M. Peng, S. Goswami, Inorg. Chem. 41 (2002) 7125.
[24] S. Jasimuddin, T. Mathur, C. Sinha, Inorg. Chim. Acta 358 (2005) 3601.
[25] P. Didier, I. Ortmans, A.K.D. Mesmacker, R.J. Watts, Inorg. Chem. 32 (1993) 5239.
[26] B.P. Sulliran, D.J. Salmon, T.J. Meyer, Inorg. Chem. 17 (1978) 3334.
[27] M.A. Bennett, T.N. Huang, T.W. Matheson, A.K. Smith, Inorg. Synth. 21 (1982) 74.
[28] M.A. Bennett, T.W. Matheson, G.B. Robertson, A.K. Smith, P.A. Tucker, Inorg. Chem. 19 (1980) 1014.
[29] M.A. Bennett, A.K. Smith, J. Chem. Soc., Dalton Trans. (1974) 233.
[30] J.W. Kang, K. Moseley, P.M. Maitlis, J. Am. Chem. Soc. 91 (1969) 5970.
[31] C. White, A. Yates, P.M. Maitlis, Inorg. Synth. 29 (1992) 228.
[32] M.I. Bruce, N.J. Windsor, Aust. J. Chem. 30 (1977) 1601.
[33] P.W. Wanandi, T.D. Tilley, Organometallics 16 (1997) 4299.
[34] M.I. Bruce, P.J. Low, B.W. Skelton, E.R.T. Tiekink, A. Werth, A.H. White, Aust. J. Chem. 48 (1995) 1887.
[35] M.I. Bruce, B.C. Hall, N.N. Zaitseva, B.W. Skelton, A.H. White, J. Chem. Soc., Dalton Trans. (1998) 1793.
[36] L.A. Oro, M.A. Ciriano, M. Campo, C. Foces-Foces, F.H. Cano, J. Organomet. Chem. 289 (1995) 117.
[37] G.M. Sheldrick, Acta Crystallogr. A64 (2008) 112.
[38] L.J. Farrugia, J. Appl. Crystallogr. 30 (1997) 565.